

Symmetric Molecular Dynamics

Sam Cox¹ and Andrew D. White^{1,*}

¹*Department of Chemical Engineering, University of Rochester*

(Dated: April 5, 2022)

We derive a formulation of molecular dynamics that generates only symmetric configurations. We implement it for all 2D planar and 3D space groups. An atlas of 2D Lennard-Jones crystals under all planar groups is created with symmetric molecular dynamics.

I. INTRODUCTION

Molecular dynamics has long been proposed as a method for predicting or understanding crystal structures[1]. However, any practitioner will confess it is near impossible to observe point group symmetries in molecular dynamics. Here we derive a constraint formulation of molecular dynamics where the symmetry group is an *input*. There is a finite number of symmetry groups. We simply simulate under all symmetry groups to generate symmetric structures.

The idea of symmetric molecular dynamics is unknown to us. The closest examples are methods like symmetry *restraints*[2]. These harmonic restraints generally keep the system close to symmetric, but no single configuration is actually symmetric. Symmetry has certainly been considered as a *measure* of molecular configurations. For example, Zabrodsky *et al.* [3] proposed a continuous symmetry measure, which is used to quantify the symmetry of atoms. In the context of spectroscopy, Hamiltonians are often constructed with specific symmetry groups[4, 5]. And of course, the direct use of symmetry for crystal structure prediction with Monte Carlo is common[6, 7].

There are two key ideas to our formulation that correspond to the two components of a space group: the point group symmetry and the Bravais lattice. The point group symmetry is treated as a holonomic constraint. The constraint equation is a function of positions that is zero when the positions are symmetric. Holonomic constraints are a relatively solved problem and we follow previous approaches[8–13]. The Bravais lattice is a constraint on the simulation lattice vectors that ensures the point group will tile space. Namely, the Bravais lattice specifies the relative lattice vector magnitudes and directions. We ensure our simulations are consistent by working in an unconstrained lattice vector space that is mapped to the correct Bravais lattice via a pre-computed tensor. This frees us to use any NPT method in the unconstrained lattice vector space while still matching the Bravais lattice.

There is little previous literature on these two ideas. The closest may be periodic boundary conditions, which cause a simulation to tile space[14]. Some symmetric boundary conditions have been implemented in the

form of rotational symmetry boundary conditions[15] and more general approaches[16, 17]. However, they do not have point group symmetries, nor do they go to the very small unit cells like we propose here.

Below we derive our equations of motion and discuss implementation details. To assess the method, we show that it conserves energy and is capable of working in arbitrary space groups. Then we demonstrate its use to enumerate crystal structures of the Lennard-Jones potential under all planar groups with NPT simulations.

II. THEORY

A. Equation of Motion

Consider the dynamics of N indistinguishable particles in D dimensions under a Hamiltonian $H(\vec{p}(t), \vec{q}(t))$. We wish to constrain H so that $\vec{q}(t)$ is symmetric at all times. Symmetry is a property of $\vec{q}(t)$ and a specific symmetry group of position transformations G , like mirror along the x axis. $\vec{q}(t)$ is point group symmetric if applying any element of the group results in no change to the positions (ignoring ordering of particles):

$$g \cdot \vec{q}(t) \sim \vec{q}(t), \forall g \in G \quad (1)$$

where $g \cdot$ means applying the group element to each particle individually, \sim means row equivalence, and G is a finite group. Group elements are represented as affine matrices in space and planar groups.

Equation 1 may hold trivially. For example, all particles are at the origin. Such special positions that are invariant to group elements are known as special Wyckoff positions[18]. We remove this assumption in Section II C, but for now additionally assume

$$g \cdot \vec{q}_i(t) = \vec{q}_i(t) \quad \text{iff } g = I \quad (2)$$

where I is the identity transformation.

Assuming Equations 1 and 2 hold at $t = 0$, the particles can be partitioned into $N/|G| = n$ group orbits. A group orbit is the set generated by applying all elements of group G to positions $\vec{q}_i(t)$

$$G[\vec{q}_i(t)] = \{g_j \cdot \vec{q}_i(t), g_j \in G\} \quad (3)$$

* andrew.white@rochester.edu

One member of all orbits will be $\vec{q}_i(t)$ itself, because G contains the identity element. We can label the particles as $q_{ij}(t)$ where i indicates the orbit and j indicates the group element. In crystallography the \vec{q}_{i0} particles are called the asymmetric unit. We can satisfy Equation 1 at all t by specifying the following holonomic constraint:

$$\sigma(\vec{q}_{ij}) = g_j \cdot \vec{q}_{i0} - \vec{q}_{ij} = \vec{0} \quad (4)$$

There are $|G| - 1$ of these constraints per group orbit and each removes D degrees of freedom. This means the degrees of freedom of the dynamics is $D \times (n - 1)$. We can simulate dynamics under the holonomic constraints by simply only modeling the asymmetric unit — they are the generalized coordinates.[19]

Thus, our algorithm is to only integrate the asymmetric unit and explicitly consider the remaining $(N - n)$ particles only when computing forces. Practically this is done by setting these constrained particles positions just before computing forces. Similar to work on periodic boundary conditions, these equations of motion may lead to linear momentum conservation problems[20, 21].

One feature of nearly all potentials used in molecular dynamics is that they are G -invariant, where G is any planar, space, or permutation group: $U(g \cdot \vec{q}) = U(\vec{q})$. That makes the forces, $F(\vec{q})$, G -equivariant:

$$F(g \cdot \vec{q}) = -g \cdot \nabla U(\vec{q}) \quad (5)$$

because the potentials are composed of angles and distances, which are invariant to rotations, mirrors, and permutations[22, 23]. For a pairwise potential, we can use Equations 3 and 5 to rewrite the potential as

$$\begin{aligned} U(\vec{q}) &= \sum_{i < j} u(\vec{q}_i - \vec{q}_j) \\ &= \frac{|G|}{2} \sum_{i=0}^n \sum_{j=1}^{|G|} u(\vec{q}_{i0} - \vec{q}_{ij}) + |G| \sum_{i=0}^n \sum_{k=i+1}^n \sum_{j=0}^{|G|} u(\vec{q}_{i0} - \vec{q}_{kj}) \end{aligned} \quad (6)$$

where the $|G|$ factor accounts for intra-group orbit interactions that are not explicitly computed. This translates an algorithm of an outer loop over the asymmetric unit and an inner loop over all particles.

B. Bravais Lattice

A space group consists of both a point group and a Bravais lattice. The Bravais lattice is specified with D D -dimensional unit cell vectors. Particles always remain in one cell among the lattice cells, which are called images. For example, we could simulate the “root” cell

and its 26 neighboring cells in 3 dimensions. We follow the approach above and treat each image of the system with virtual particles while only integrating the root cell. This means all images of the system are explicit and we can violate the minimum image convention. We were not signatories of the minimum image convention anyway. This approach allows the cell vectors to shrink well below the distance cut-off of the potential, provided we have enough virtual particles to populate past the cut-off of the asymmetric unit of the origin cell. You can simulate 3^{aD} images to allow the cells to shrink to at least $1/a$ the cut-off distance.

We need to convert between the fractional coordinates, which are used to tile the particles and apply the point group symmetry, to the Cartesian coordinates, which are used for integration and computed potentials. Given the box vectors in row-form B , we can transform between the representations via

$$\vec{s}(t) = B^{-1}\vec{q}(t), \quad \vec{q}(t) = B\vec{s}(t) \quad (7)$$

where $s(t)$ is the fraction of each lattice vector (i.e., fractional coordinates). Wrapping is trivial with fractional coordinates: $s(t) \bmod 1.0$ will wrap the coordinates. All point group transformations are applied in $\vec{s}(t)$, however a B^{-1} term should be added to Equation 3 so that it operates on fractional coordinates.

Bravais lattices include more than just the usual cubic and triclinic lattices commonly seen in molecular dynamics barostats. To ensure the cell vectors are consistent with the Bravais lattice while changing box size, we define a tensor \mathbf{L} of shape $D \times D \times D \times D$ that maps from a triclinic box vectors to the proper Bravais Lattice box vectors of the space group. For example, L_{2011} is the contribution to Bravais lattice vector 2’s x component from triclinic box vector 1’s y component. There are many choices that could be made for \mathbf{L} . For example, to make a cubic Bravais lattice from a triclinic box vector we require a single parameter a to define the three lattice vectors $(a, 0, 0)$, $(0, a, 0)$, $(0, 0, a)$. We could set a by averaging all the vector lengths, averaging all vector components, or select a to be the first element of the first vector. Each of these choices gives a different \mathbf{L} and some have large null spaces. NPT is then accomplished via scaling Monte Carlo moves in the triclinic box vectors (B') following Frenkel and Eppenga [24] and the proper Bravais Lattice is computed via $B = \mathbf{L}B'$.

C. Wyckoff Positions

It is possible to have particles that violate Equation 2 while still satisfying Equation 1 if q_{i0} is in a special position called a Wyckoff position — like the origin[18]. To perform constrained molecular dynamics of particle $q_{i0}(t)$ occupying a Wyckoff position, we define a subgroup G' that contains the elements of G which do not leave $q_{i0}(t)$ invariant plus an identity group element. The identity of

this subgroup is not the identity transform, but instead a transform that projects from a general position into the Wyckoff position. For example, the Wyckoff position may be the vertical line $x = 0$ and the identity group element would be the transform $x' = 0, y' = y$. We will denote this group element as P to hint it is a projection.

The group orbit is similarly defined on the subgroup and the other procedures above apply. However, $q_{i0}(t)$ must stay in a Wyckoff position at all time to satisfy Equation 1. This can be accomplished via traditional constrained molecular dynamics of Lagrange multipliers [25]. Omitting the indices on $\vec{q}_{i0}(t)$, our holonomic constraint is:

$$\sigma[\vec{q}(t)] = P\vec{q}(t) - \vec{q}(t) = \vec{0} \quad (8)$$

and the force from the constraint will be

$$\vec{F}_c = \vec{\lambda}J[g] = \vec{\lambda}(P - I) \quad (9)$$

where $J[\sigma]$ is the Jacobian of σ with respect to constraint dimension and element of $\vec{q}(t)$. We can solve for $\vec{\lambda}$ by knowing that $\sigma[\vec{q}(t + \Delta t)] = \vec{0}$:

$$\vec{\lambda} = \frac{\Delta t^2}{m} [(P - I)^2]^{-1} \sigma[\vec{q}'(t + \Delta t)] \quad (10)$$

where Δt is the timestep, m is the mass of the particle, and $\vec{q}'(t + \Delta t)$ is $\vec{q}(t)$ integrated without the constraint force by Δt . All terms are constant except $g[\vec{q}'(t + \Delta t)]$, which simplifies computation.

III. METHODS

We use the BAOAB Langevin dynamics integrator described in [26, 27]. Equation 4 is applied during position updates and Equation 3 is applied before velocity updates (force computation). All simulations are Lennard-Jones potentials with cutoff 3.5 and in reduced units. NVE simulations are conducted with the velocity-verlet integrator. A timestep of 0.005 and a Langvin γ of 0.1 were used for all simulations. Since images are explicit in our implementation, it is necessary to specify the number. We use an image radius of 2 – meaning 3^{2D} images are simulated where D is the dimension. To generate starting configurations, points were randomly generated and filtered to fit into the space group asymmetric unit as specified by Aroyo [28]. Point group generators and Wyckoff sites were taken from Bilbao crystallography server[29–31].

IV. RESULTS

We first consider if our implementation conserves energy. Figure 1 show the total energy of NVE simulations

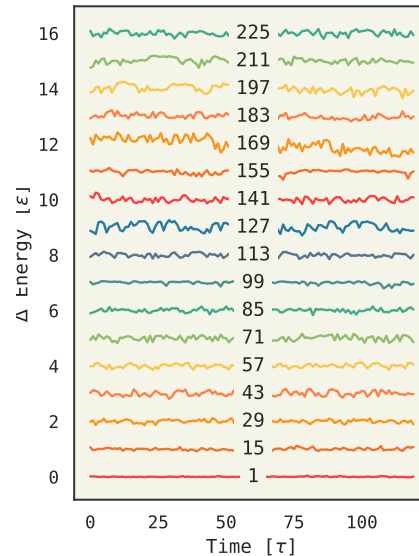


FIG. 1. Total energy from NVE simulations under different symmetry groups in 3D. Groups are indicated with Hall numbers. 5 particles are in the asymmetric unit and the simulations are at a number density of 0.2 and starting temperature of 0.5. The increase of fluctuations is because the unit cell (total particles) increases with size of symmetry group.

under a subset of space groups with 5 particles in the asymmetric unit. These were done at number densities of 0.2, with starting temperature 0.5, and for 30k timesteps. The bottom trace (P1) has no symmetry constraints and shows good conservation. There are more fluctuations at other symmetry groups because there are more particles in their unit cells and thus higher energy fluctuations. For example, space group 127 (P4/mbm) has 80 particles in a unit cell when there are 5 in the asymmetric unit.

Figure 2 shows an enumeration of crystal structures under different symmetry groups for a 2D Lennard-Jones fluid. The structures are generated in 2 steps. First, we simulate under a symmetry group constraint in NPT ($P = 0.25, T = 0.1$) for 1M steps. Next, we do a constrained equilibration under NVT for 100k steps at $T = 0.05$. This structure is then the proposed crystal structure for the given symmetry group. Figure 2 shows the root mean squared deviation (RMSD) if the resultant structure is simulated under no symmetry constraint in NVE for 5k steps. The assumption is that if the structure does not collapse (RMSD rise), it is meta-stable. We indeed find that this protocol under no symmetry constraints (p1) gives the correct hexagonal packing.

To enumerate all planar groups in 2D, we simulate under each group, with 4 choices of particle number (in unit cell), and varying occupancy of Wyckoff sites. As expected, the planar groups with hexagonal Bravais lat-

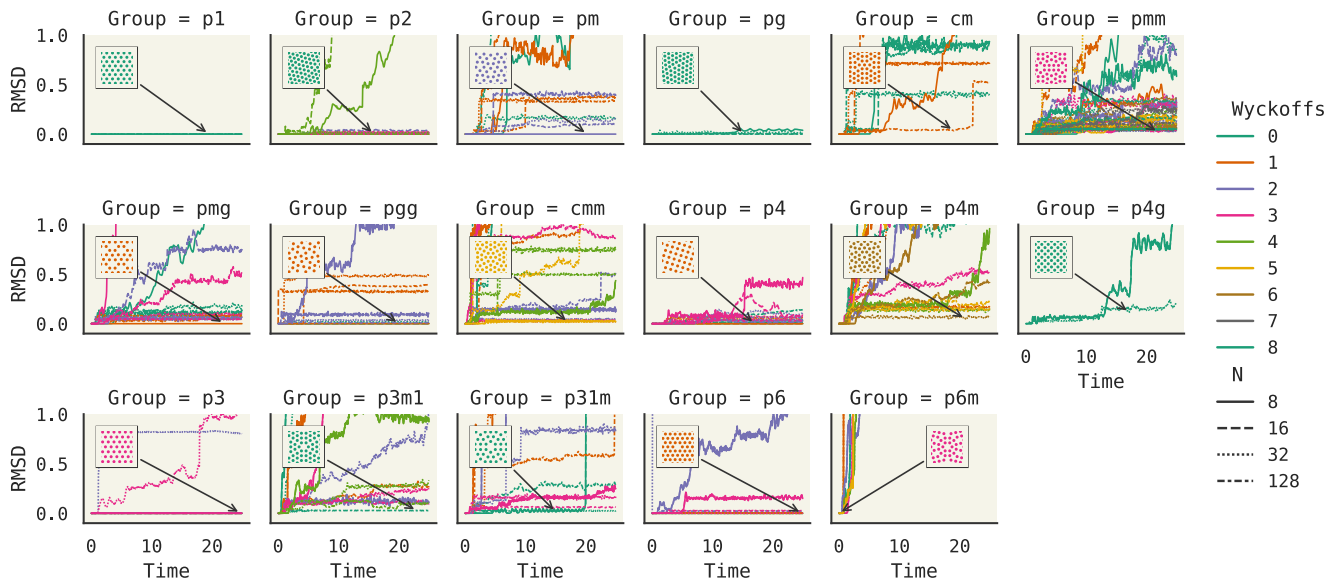


FIG. 2. An atlas of 258 Lennard-Jones crystal structures. Subplots are broken down by planar group and each line color/style indicates Wyckoff occupancy and unit cell particle count. Individual plots show RMSD from starting configuration, which was constrained to match the planar group in subplot titles. RMSD was calculated during NVE simulation of 5k steps with no symmetry constraints. A rise indicates change of configuration – meaning the starting configuration was not stable. Missing traces indicate either simulation diverged or number density did not exceed 0.5.

tices (or permit them) have stable structures: p1, p2, pg, p3, p6, and cmm[32]. Some unusual stable structures are seen without hexagonal close-packing like p4m and p3m1. Meta-stable structures like these would be nearly impossible to generate without symmetry constraints in molecular dynamics.

V. CONCLUSIONS

We have formulated a symmetric molecular dynamics algorithm and implemented it. Results show

that it can do NPT to enumerate meta-stable crystal structures. A reference implementation is available at <https://github.com/whitead/symd>, although the method is simple enough that it can be implemented in other simulation engines.

VI. ACKNOWLEDGEMENTS

This work was supported by the NSF under grant 1751471. We thank Prof. Glen Hocky and Dr. Charles Matthews for valuable discussion and feedback.

-
- [1] M. Parrinello and A. Rahman, Polymorphic transitions in single crystals: A new molecular dynamics method, *Journal of Applied physics* **52**, 7182 (1981).
 - [2] A. Anishkin, A. L. Milac, and H. R. Guy, Symmetry-restrained molecular dynamics simulations improve homology models of potassium channels, *Proteins: Structure, Function, and Bioinformatics* **78**, 932 (2010).
 - [3] H. Zabrodsky, S. Peleg, and D. Avnir, Continuous symmetry measures, *Journal of the American Chemical Society* **114**, 7843 (1992).
 - [4] A. V. Burenin, The “chain of symmetry groups” concept in the theory of molecular spectra, *Physics-Uspekhi* **36**, 177 (1993).
 - [5] P. R. Bunker and P. Jensen, *Molecular symmetry and spectroscopy*, Vol. 46853 (NRC research press, 2006).
 - [6] B. P. van Eijck and J. Kroon, Upack program package for crystal structure prediction: Force fields and crystal structure generation for small carbohydrate molecules, *Journal of computational chemistry* **20**, 799 (1999).
 - [7] S. Fredericks, K. Parrish, D. Sayre, and Q. Zhu, Pyxtal: A python library for crystal structure generation and symmetry analysis, *Computer Physics Communications* **261**, 107810 (2021).
 - [8] J.-P. Ryckaert, G. Ciccotti, and H. J. Berendsen, Numerical integration of the cartesian equations of motion of a system with constraints: molecular dynamics of n-alkanes, *Journal of computational physics* **23**, 327 (1977).
 - [9] H. C. Andersen, Rattle: A “velocity” version of the shake algorithm for molecular dynamics calculations, *Journal of computational Physics* **52**, 24 (1983).

- [10] D. J. Tobias and C. L. Brooks III, Molecular dynamics with internal coordinate constraints, *The Journal of chemical physics* **89**, 5115 (1988).
- [11] J.-P. Ryckaert, Special geometrical constraints in the molecular dynamics of chain molecules, *Molecular Physics* **55**, 549 (1985).
- [12] R. Edberg, D. J. Evans, and G. Morriss, Constrained molecular dynamics: Simulations of liquid alkanes with a new algorithm, *The Journal of chemical physics* **84**, 6933 (1986).
- [13] G. Ciccotti and J.-P. Ryckaert, Molecular dynamics simulation of rigid molecules, *Computer Physics Reports* **4**, 346 (1986).
- [14] T. Hansson, C. Oostenbrink, and W. van Gunsteren, Molecular dynamics simulations, *Current opinion in structural biology* **12**, 190 (2002).
- [15] A. Roy and C. B. Post, Microscopic symmetry imposed by rotational symmetry boundary conditions in molecular dynamics simulation, *Journal of chemical theory and computation* **7**, 3346 (2011).
- [16] R. Denton and Y. Hu, Symmetry boundary conditions, *Journal of Computational Physics* **228**, 4823 (2009).
- [17] G. J. Wagner, E. G. Karpov, and W. K. Liu, Molecular dynamics boundary conditions for regular crystal lattices, *Computer Methods in Applied Mechanics and Engineering* **193**, 1579 (2004).
- [18] R. W. G. Wyckoff, *The Analytical Expression of the Results of the Theory of Space-groups*, 318 (Carnegie institution of Washington, 1922).
- [19] You can also arrive at this solution by constraining the Cartesian coordinates and finding Lagrange multipliers.
- [20] R. B. Shirts, S. R. Burt, and A. M. Johnson, Periodic boundary condition induced breakdown of the equipartition principle and other kinetic effects of finite sample size in classical hard-sphere molecular dynamics simulation, *The Journal of chemical physics* **125**, 164102 (2006).
- [21] V. A. Kuzkin, On angular momentum balance for particle systems with periodic boundary conditions, *ZAMM-Journal of Applied Mathematics and Mechanics/Zeitschrift für Angewandte Mathematik und Mechanik* **95**, 1290 (2015).
- [22] F. Musil, A. Grisafi, A. P. Bartók, C. Ortner, G. Csányi, and M. Ceriotti, Physics-inspired structural representations for molecules and materials, *Chemical Reviews* **121**, 9759 (2021).
- [23] A. D. White, *Deep Learning for Molecules and Materials* (2021).
- [24] D. Frenkel and R. Eppenga, Monte carlo study of the isotropic-nematic transition in a fluid of thin hard disks, *Physical review letters* **49**, 1089 (1982).
- [25] S. Miyamoto and P. A. Kollman, Settle: An analytical version of the shake and rattle algorithm for rigid water models, *Journal of computational chemistry* **13**, 952 (1992).
- [26] B. Leimkuhler and C. Matthews, Robust and efficient configurational molecular sampling via langevin dynamics, *The Journal of chemical physics* **138**, 05B601-1 (2013).
- [27] B. Leimkuhler and C. Matthews, Efficient molecular dynamics using geodesic integration and solvent-solute splitting, *Proceedings of the Royal Society A: Mathematical, Physical and Engineering Sciences* **472**, 20160138 (2016).
- [28] M. I. Aroyo, *International Tables for Crystallography* (Wiley Online Library, 2013).
- [29] M. I. Aroyo, J. Perez-Mato, D. Orobengoa, E. Tasci, G. de la Flor, and A. Kirov, Crystallography online: Bilbao crystallographic server, *Bulg. Chem. Commun* **43**, 183 (2011).
- [30] M. I. Aroyo, J. M. Perez-Mato, C. Capillas, E. Kroumova, S. Ivantchev, G. Madariaga, A. Kirov, and H. Wondratschek, Bilbao crystallographic server: I. databases and crystallographic computing programs, *Zeitschrift für Kristallographie-Crystalline Materials* **221**, 15 (2006).
- [31] M. I. Aroyo, A. Kirov, C. Capillas, J. Perez-Mato, and H. Wondratschek, Bilbao crystallographic server. ii. representations of crystallographic point groups and space groups, *Acta Crystallographica Section A: Foundations of Crystallography* **62**, 115 (2006).
- [32] This depends on Wyckoff site occupancy too.